RSC Advances

ROYAL SOCIETY OF CHEMISTRY

www.rsc.org/advances

Well-defined triblock copolymers with photolabile middle block of poly(phenyl vinyl ketone): Facile synthesis, chain-scission mechanism and controllable photocleavability

Ruiwei Guo, Pengbo Mei, Qing Zhong, Yuan Yao, Qian Su, Jianhua Zhang*

Department of Polymer Science and Engineering, School of Chemical Engineering and Technology, Tianjin University, Tianjin, 300072, China

Corresponding author:

Jianhua Zhang

E-mail address: jhuazhang@tju.edu.cn; Tel.: +862 227 402 364; Fax: +862 227 890 710.

Department of Polymer Science and Engineering, School of Chemical Engineering and Technology, Tianjin University, Tianjin, 300072, China

Supporting information

Synthesis process and ^{1}HNMR of PVK; ^{1}HNMR and FTIR spectrum of PSt-PPVK-PAA; ^{1}HNMR spectrum and GPC curves of PPVK; UV curves of BCCD, St, PSt prepared by BCCD, PMK, PVK and PPVK prepared by BCCD; Size and size distribution of PSt-PPVK-PAA self-assembled micelles

Abstract

The effective preparation of the photoresponsive polymers with precisely controlled location and number of photolabile units in the main chain is essential for their applications. In this study, a series of photocleavable well-defined triblock copolymers with the photocleavable middle block of poly(phenyl vinyl ketone) (PPVK) were readily synthesized by RAFT polymerization. The chain structure and chemical composition of copolymers were characterized by ^{1}HNMR, FTIR and GPC. The well-controlled molecular weights and low polydispersity (< 1.30) demonstrated the excellent controllability and living characteristics of RAFT process to the polymerization of PVK. And then the photocleavage mechanism and kinetics of PPVK-functionalized copolymers were systematically investigated by tracking, fractionating and quantifying the photolysis products using gradient polymer elution chromatography (GPEC). The results not only confirmed the rapid photocleavability of PPVK-based polymers, but also firstly provided the direct evidence for the proposed Norrish type reaction mechanism of the chain scission of PPVK. Moreover, the investigation of the effect of PPVK chain on the photolysis kinetics demonstrated the photodegradation rate of PPVK-based polymers can be controlled by adjusting the PPVK chain length in block copolymers. As a preliminary application study, the self-assembled micelles of the obtained PPVK-based amphiphilic polymers under light irradiation were found to undergo photo-triggered rapid disassembly and exhibited photo-controllable emulsifiability. In sum, the incorporation of the high photolabile PPVK into block copolymers by RAFT polymerization provides a promising strategy for the construction of complex polymeric architectures or nanostructures with controllable photocleavability.

Introduction

In the past several decades, tremendous attention has been paid to the field of stimuli-responsive polymers, which are able to undergo reversible or irreversible changes in chemical structures and/or physical properties in response to an external stimulus, such as pH, heat, enzyme, photo irradiation, electric and magnetic fields, and external additives (ions, bioactive molecules, etc.).[1-4] Among these stimuli, the use of light irradiation is particularly attractive due to its easy operation, low cost, non-invasive nature, remote controllability, high spatial resolution and temporal precision.[3-5] As a result, photosensitive polymers, especially photocleavable polymers, which can be degraded into smaller molecular fragments upon light irradiation, hold great potential for many applications in broad fields, including drug delivery, surface patterning, structural stabilization, pharmaceutical formulation and environment science.[3-10]

Generally, photocleavable polymers can be classified into side-chain-type polymer and main-chain-type polymer. For the former, the photoremovable groups, such as O-nitrobenzyl (ONB), nitrophenethyl, and their dimethoxy derivatives, are positioned in the side-chain as pendants.[11,12] For example, the photosensitive polymers bearing photolabile side groups can be readily prepared by free radical polymerization of ONB-functionalized vinyl monomers.[13,14] While for the latter, single or multiple photolabile species are covalently catenated into the chain backbone.[12,15] Compared with side-chain-type photosensitive polymers, the main-chain-type polymers and their corresponding self-assembled nanostructures should undergo more severe disruption

and more dramatic change in structure, morphology or property upon light irradiation, allowing for more sophisticated applications and thus gaining more attention.[9, 12, 15] One of the most common methods for the incorporation of photocleavable groups into polymer main chains is the use of functional initiators or transfer agents.[12,15] Zhao et al applied ONB-functionalized macro-RAFT agents to prepare a series of main-chain-type block polymers with a photocleavable ONB ester junction.[16,17] However, this strategy is often constrained, due to the extreme difficulty in synthesis of these commercially unavailable functional reagents and their limited incorporating ability. The post-polymerization modification by a photocleavable linker is another important approach, which also suffers from rigorous synthetic requirements, low efficiency and uncontrollable process.[12,15,18]

Comparatively, direct polymerization of functional monomers clearly is a more attractive strategy, especially considering the emergence of living/controlled radical polymerization (LRP) techniques such as reversible addition-fragmentation chain transfer (RAFT), atom-transfer radical polymerization (ATRP) and nitroxide-mediated polymerization (NMP), which have been proved to be a powerful platform to synthesize well-defined polymers with controlled chain architecture, designed composition, and predetermined molecular weight.[19,20] The direct polymerization of photocleavable monomers not only can readily yield very high functional group densities in the polymer backbone, leading to a significant increase in photosensitivity and degradation rate, but also can precisely control the location of multiple photocleavable units and construct complex chain architecture by combining

techniques of living/controlled radical polymerization.[15,21] Nevertheless, the functional vinyl monomers containing photosensitive groups, such as the most common nitrobenzyl and azobenzene groups, can exert the inhibition effect to the free radicals.[22-24]

Polymers based on vinyl ketone monomers, especially phenyl vinyl ketone (PVK) and methyl vinyl ketone (MVK), were representative photoresponsive polymers with high photocleavability. Many researchers have studied in detail their photochemical behaviors and proposed the Norrish type reaction mechanism for the main-chain scission of vinyl ketone-based polymers.[25-29] These polymers have been used as packing materials[30] and functional film materials[10], which are generally prepared without accurate structural control by conventional free radical polymerization. Evidently, the well-defined vinyl ketone-based polymers with precisely controlled location and number of photocleavable units in the main chain are required in order to broaden their applications. As mentioned above, LRP is the most efficient and powerful synthetic tool for the preparation of well-defined polymers. However, due to unfavorable coordination between the monomer and metal catalyst, the ATRP polymerization of MVK was found to suffer from significant restrictions.[31] And Hepperle et al. also showed that NMP polymerization exhibited a very low control activity to vinyl ketone monomers.[32] Comparatively, RAFT process as a metal-free and homogeneous polymerization has proved to be the most versatile and robust LRP, because it is applicable to a wide range of monomers and reaction conditions.[33-35] However, quite surprisingly, to the best of our knowledge, except a preliminary study

carried out by Cheng et al,[21] there appears to be no study that has focused on the preparation of well-defined vinyl ketone-based photocleavable polymers and the corresponding photolysis mechanism.

In this study, the photodegradable triblock copolymers with PPVK as the middle block, including various polystyrene-*b*-poly(phenyl vinyl ketone)-*b*-polymethyl acrylate (PSt-PPVK-PMA) and amphiphilic polystyrene-*b*-poly(phenyl vinyl ketone)-*b*-polyacrylic acid (PSt-PPVK-PAA), were synthesized by RAFT polymerization. And then the photocleavage mechanism and kinetics of PSt-PPVK-PMA were systematically investigated by using gradient polymer elution chromatography (GPEC). GPEC has been proven to be able to fractionate the chemically heterogeneous polymers on the basis of the differences in solubility and specific column interactions of polymers.[35-39] The photodegradation behavior of PSt-PPVK-PMA under light irradiation was demonstrated by photo-induced disintegration of micelles and photo-controllable demulsification of W/O miniemulsion. The results obtained here are expected to provide a photosensitive platform for potential applications in environmental, biological and medicinal fields.

Materials and methods

Materials

Phenyl methyl ketone (PMK), trifluoroacetic acid (TFA), diisopropylamine (DIPA) and paraformaldehyde (POM) were purchased from Aladdin Industrial Corporation (Shanghai, China) and used as received. According to a modified method,[40] the monomer phenyl vinyl ketone (PVK) was prepared by a *a*-methylenation reaction between PMK and POM by using the salt complex of DIPA:TFA as catalyzer. The detailed information and ^{1}HNMR characterization were given in **Figure S1** in the Supporting Information. The RAFT agent benzyl 9H-carbazole-9-carbodithioate (BCCD) was synthesized according to our previous study.[41] HPLC grade tetrahydrofuran (THF), 1, 2-dichloroethane (DCE) and acetonitrile (ACN) were purchased from Merck (Darmstadt, Germany). Styrene (St), acrylic acid (AA), methyl acrylate (MA) and 2, 2'-azobis(isobutyronitrile) (AIBN) were obtained from Jiangtian Chemical Reagents Co., Ltd. (Tianjin, China). St and MA were washed with an aqueous solution of NaOH (5%) and fractionally distilled under vacuum to remove inhibitor and polymer. AA and AIBN were purified by recrystallization. All other reagents were commercially available from Jiangtian Chemical Reagents Co., Ltd. (Tianjin, China) and used as received.

Synthesis of photocleavable triblock copolymers by RAFT polymerization

The photodegradable triblock copolymers with PPVK as the middle block, including various polystyrene-*b*-poly(phenyl vinyl ketone)-*b*-polymethyl acrylate (PSt-PPVK-PMA) and amphiphilic polystyrene-*b*-poly(phenyl vinyl ketone)-b-polyacrylic acid (PSt-PPVK-PAA), were synthesized by a three-step

sequential RAFT polymerization as shown in **Scheme 1**. As the first block, the polymer PSt with pre-ordained polymerization degree was prepared in the presence of BCCD as RAFT agent and AIBN as initiator in THF. And then it was used as macro-RAFT agent in the subsequent polymerization to prepare well-defined PSt-PPVK with different chain length of PPVK, which can be further used as RAFT agent to prepare the triblock PSt-PPVK-PMA and PSt-PPVK-PAA, respectively. A typical polymerization procedure was as follows. The dry vessel was loaded with St (15.6 g, 150 mmol), BCCD (0.333 g, 1.0 mmol), AIBN (0.0413 g, 0.25 mmol) and then diluted up to 50 mL with THF. After complete dissolution, the solution was thoroughly deoxygenated by purging with nitrogen for 20 min. Subsequently, the air-tight sealed vessel was placed in a thermostatic water bath at 60 ^{o}C for 8 h under nitrogen atmosphere and in the dark condition. The resulting reaction solution was precipitated into a large quantity of diethyl ether. The PSt was collected by filtration and dried in a vacuum oven at 50 ^{o}C. The monomer conversion was determined gravimetrically to about 61%. The molecular weight of PSt was determined by GPC analysis and ^{1}HNMR data via comparing the intensity of characteristic resonance of the carbazyl proton resonances (7.99 ~ 8.13 ppm and 8.34 ~ 8.48 ppm) of BCCD to that of methylene proton resonances at 1.18 ~ 1.72 ppm of PSt. The PSt (M_n = 9.88 $\times 10^3$ Da calculated from ^{1}HNMR data, the number-average degrees of polymerization (DP_n) $\approx$ 92) as macro-RAFT agent was chain extended by PVK to obtain PSt-PPVK under a condition similar to that for PSt. The PPVK content in PSt-PPVK were controlled by the initial molar mass ratio of monomer to macro-RAFT agent and

monomer conversion. Three different PSt-PPVK with theoretical DP_n of PPVK = 5, 10 and 30, respectively, was designed and prepared. The resultant PSt-PPVK copolymers were determined by GPC and ^{1}HNMR. The DP_n of PPVK block in PSt-PPVK can be calculated by comparing the peak area of aromatic proton resonances (6.45 ~ 7.30 ppm) of PSt and PPVK to that of methylidyne protons at 2.70 ~ 3.40 ppm of PPVK. Under similar polymerization condition, the triblock copolymers PSt-PPVK-PMA with similar chain length of PMA were prepared by use of the obtained PSt-PPVK as macro-RAFT agent. MA was used as the third monomer, as PMA segments have not UV absorbance above 240 nm, facilitating GPEC experiments.[35] The composition and structure of PSt-PPVK-PMA were determined by GPC, FTIR and ^{1}HNMR, and the content of PMA block was calculated by comparing the peak area of aromatic proton resonances (6.45 ~ 7.30 ppm) of PSt to that of methyl proton resonances (3.60 ~ 3.85 ppm) of PMA. The detailed characterization data for all triblock copolymers are given in **Table 1**. In order to study the photocleavable behavior of PPVK-based triblock copolymers micelles, the amphiphilic triblock copolymers PSt-PPVK-PAA were prepared via RAFT polymerization by using PSt-PPVK as macro-RAFT agent under approximately the same conditions for PSt-PPVK-PMA. The composition and chemical structure of PSt-PPVK-PAA were determined by ^{1}HNMR and FTIR, as shown in **Figure S2** and **S3** in Supporting Information. And the DP_n of PAA block was calculated by comparing the peak area of aromatic proton resonances (6.45 ~ 7.30 ppm) of PSt to that of methylidyne protons at 2.00 ~ 2.54 ppm of PAA. In addition, PPVK with DP_n

of about 50 as a standard sample for GPEC analysis was also prepared by RAFT polymerization according to the same homopolymerization procedure of PSt, and the ^{1}HNMR and GPC of PPVK were given in **Figure S4** and **Figure S5** in Supporting Information. All polymerization experiments were carried out in the dark condition and the obtained polymers were stored without light exposure.

Conversion (*Conv.*) was determined by gravimetrical method and was calculated based on Eq.(1):

$$Conv. = \frac{W_P - W_{RAFT}}{W_m} \times 100\% \qquad (1)$$

where, W_p, W_{RAFT} and W_m respectively stand for the weight of the polymer, initial weight of RAFT agent and monomer.

And the theoretical molecular weight ($M_{n,th}$) of polymers was calculated according to Eq.(2):

$$M_{n,th} = \frac{W_m}{m_{RAFT}} \times Conv. + M_{RAFT} \qquad (2)$$

where, W_m, m_{RAFT} and M_{RAFT} are the weight of monomer in the feed, the initial mole of RAFT agent added and the molecular weight of RAFT agent, respectively.

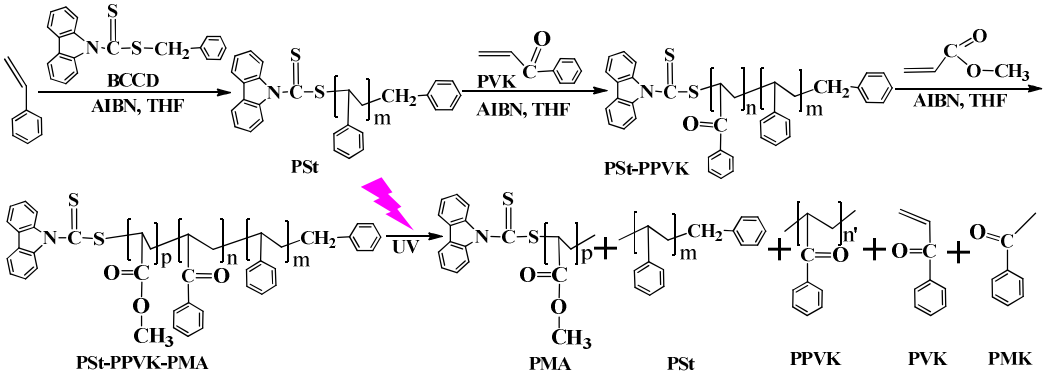

Scheme 1. Synthesis process and proposed photocleavage mechanism of PSt-PPVK-PMA

Preparation and characterization of PSt-PPVK-PAA micelles

PSt-PPVK-PAA copolymer micelles were prepared by a nanoprecipitation method. Typically, the copolymer PSt_{92}-$PPVK_{11}$-PAA_{26} (2.0 mg) was dissolved in 1.0 mL THF. And then 1 mL of deionized water was added into the above polymer solution at a rate of 500 μL/h under vigorous stirring. Afterwards, 9 mL of deionized water was added quickly. Then, the resulting solution was stirred overnight to allow complete evaporation of THF at room temperature. The solution with final concentration of 0.2 mg/mL was filtered through a 0.6 μm filter before use. The size and size distribution of micelles were performed by a dynamic light scattering (DLS) measurement using a laser particle size analyzer (Zetasizer Nano, Malvern, UK). The morphologies of micelles were observed under a Japan JEM-2100F transmission electron microscopy (TEM) system at an operated voltage of 200 kV. For TEM measurement, the sample was prepared by adding a drop of micelles solution onto the copper grid, and then the sample was air-dried and measured at room temperature. The atomic force microscopy (AFM) analysis was performed using a Multimode V scanning probe microscope (Veeco Metrology Group, USA), which was operated in Tapping Mode. For AFM measurements, a drop of the polymer colloidal solution was placed on a glass slide and the solution was allowed to evaporate at room temperature in the dark condition.

Photocleavage of PSt-PPVK-PMA polymers and PSt-PPVK-PAA micelles

1 mg/mL PSt-PPVK-PMA solution in DCE (or PSt-PPVK-PAA micelles in water) was prepared and placed in a quartz cuvette. The volume of assay solution in the

cuvette was 1 mL. And then the photodegradation experiments were carried out at room temperature by using a UV oven (IntelliRay 400, Uvitron International, Inc. USA) in combination with a UV filter (XUL0300, Longpass Filter/UV 300 nm, Asahi Spectra USA Inc.) to provide UV light in the range of 300 to 400 nm. The distance of sample to lamp was 14 cm, and the horizontal angle of quartz cuvette was 30^{o}. Under light intensity of 100 mW/cm^2, the samples were exposed to UV irradiation for a predetermined time. And subsequently the PSt-PPVK-PMA solutions were analyzed by GPC and GPEC, and the change of PSt-PPVK-PAA micelles after exposure to UV light was determined by TEM and AFM according to the method as mentioned above.

Miniemulsions with Photo-controllable stability by PSt-PPVK-PAA

Photosensitive stabilization of water-in-oil miniemulsions by amphiphilic PSt-PPVK-PAA was studied. Reverse emulsions were prepared by mixing 10 mL of 0.03 g/mL PSt-PPVK-PAA dimethylbenzene solution with 10 mL of 20 wt% NaCl aqueous solution under stirring with a magnetic stirrer at 500 r/min. The pH value of the emulsion was adjusted to 7.0 with NaOH solution. Then the miniemulsions were obtained by sonicating with ultrasonic cell disruptor (400 W) for 20 min in an ice bath. The obtained miniemulsions were placed into quartz cuvettes, which were kept in the dark or exposed to solar light for a pre-determined time to investigate the photo-controllable stability of miniemulsions.

Characterization

The polymer samples for UV-vis, ^{1}HNMR, FTIR and GPC analysis were purified by repeated solution/precipitation in THF/diethyl ether to remove unreacted monomer

and initiator. The UV-vis spectra were measured by WFZ-26A UV-vis spectrophotometer (Tianjin Science Instrument Plant, China) using DCE as solvent. ^{1}HNMR spectra of the products were recorded on a Varian Inova-500M instrument (Varian Inc., Palo Alto, USA) with $CDCl_3$ or CD_3COCD_3 (acetone-d6) as a solvent and tetramethylsilane (TMS) as the internal standard. Fourier transform infrared spectroscopy (FT-IR) was carried out using KBr disks in the region of 4000-500 cm^{-1} by using BIO-RAD FT-IR 3000 (BIO-RAD Company, Hercules, USA). The molecular weights and polydispersities index (PDI) of the polymers were determined with an Agilient 1100 gel permeation chromatographer (GPC) equipped with a refractive index detector, using Shodex GPC KF-803L column with molecular weight range 500– 42,000 calibrated with PSt standard samples. THF was used as eluent at a flow rate of 1.0 mL/min at 30 ^{o}C.

Gradient polymer elution chromatography

The normal phase GPEC experiments were performed with an Agilent 1100 series systems consisting of quaternary gradient pump, variable wavelength UV-detector, on-line vacuum degasser, thermostatted column compartment and autosampler with variable injection volume. The column, successfully applied for the GPEC experiments, was a Kromasil silica gel column (100Å, 150×4.6mm, 5 μm, Scienhome Science Instruments Co., Ltd. Tianjin, China). The applied solvents were HPLC grade DCE and ACN. The elution program began with an isocratic flow of DCE/ACN = 93/7 (v/v) for 1 min, followed by a linear gradient from DCE/ACN = 93/7 (v/v) to DCE/ACN = 70/30 (v/v) for 1.5 min, an isocratic flow (DCE/ACN = 70/30, v/v) for 1

min, and then a linear gradient from DCE/ACN = 70/30 (v/v) to DCE/ACN = 30/70 (v/v) for 3 min, and finally completed by an isocratic flow of DCE/ACN = 30/70 (v/v). The chromatographic system and the selected gradient elution conditions were similar to our previous studies, which the elution conditions have been proved to be effective for separation and characterization of styrene and acrylate block copolymers.[35,42] The samples were dissolved in DCE. The concentration used for GPEC detected by a UV detector at 260 nm was 1 mg/mL. The established flow was 1 mL/min and the injection volume 20 μL. The applied column temperature was 30 °C.

Data were acquired, and the relative retention time and relative peak area of each common peak in the chromatographic profile of samples were analyzed and quantified by using Agilent's ChemStation chromatography software (Agilent) and Origin™ software (OriginLab Corporation, Northampton, USA).

Results and discussion

Preparations and characterizations of triblock copolymers

Due to its high tolerance to functional groups and mild reaction conditions, RAFT process has been proved to be a facile and robust approach to synthesize sophisticated polymers with controlled chain architecture and specific functionality.[33-35] A series of well-defined triblock copolymers with middle block of PPVK were synthesized by a three-step sequential RAFT polymerization. The DP_n was controlled by the initial molar mass ratio of monomer to RAFT agent and monomer conversion. The DP_n of the first block PSt was fixed at about 92 (M_n = 9.88 × 10^3 Da, PDI = 1.12) and then the PSt was used macro-RAFT agent to prepare PSt-PPVK with different PPVK content, which can further be applied as RAFT agent to obtain triblock copolymers PSt-PPVK-PMA and amphiphilic PSt-PPVK-PAA. The chain structure and chemical composition of copolymers were characterized by ^{1}HNMR, FTIR and GPC and were shown in **Figure 1**, **Figure 2** and **Figure 3**, respectively. PSt and PSt-PPVK with similar structure both exhibited the resonance signals of methine and methylene protons in backbone (1.20-2.30 ppm) and phenyl protons (6.25-7.70 ppm). In addition, PSt-PPVK showed the characteristic signal of methine proton of PPVK at 2.70 ~ 3.40, suggesting the formation of PSt-PPVK. Compared with the spectra of PSt and PSt-PPVK, the signals at 3.60 ~ 3.85 ppm corresponding to methyl (-CH_3) of MA units were observed in the spectrum of PSt-PPVK-PMA. Typical signals of the aromatic ring and methylene appeared at 3027 cm^{-1}, 2920 cm^{-1}, 1605 cm^{-1}, 1455 cm^{-1} and 695-760 cm^{-1} in FTIR spectra of PSt and PSt-PPVK. Besides the characteristic peaks of PSt, the characteristic signals of carbonyl (C=O) in PVK units at 1680 cm^{-1}

presented in the spectrum of PSt-PPVK. On inspection of the FTIR spectra in **Figure 2**, PSt-PPVK-PMA exhibited the characteristic peaks of carbonyl (C=O) and carbon-oxygen bond in ester bonds of PMA at about 1735 cm^{-1} and 1160 cm^{-1}. These results showed that triblock copolymers PSt-PPVK-PMA were obtained. The ^{1}HNMR and FTIR of amphiphilic PSt-PPVK-PAA were given in **Figure S2** and **Figure S3** in Supporting Information, which also confirmed its structure and composition (PSt_{92}-$PPVK_{11}$-PAA_{26}). The GPC curves of PSt, PSt-PPVK and PSt-PPVK-PMA were shown in **Figure 3**. It can be found that all of polymers showed symmetrical and unimodal GPC curves with narrow molecular weight distributions (PDI < 1.30). The molecular weights that were calculated from the ^{1}HNMR data and obtained by GPC analysis were listed in **Table 1**. Moreover, it can be found that the molecular weights calculated from ^{1}HNMR were close to those obtained by GPC. The results above indicated that the RAFT polymerization possess very good controllability and can be used to prepare PPVK-functionalized polymers with controlled chain architecture and predetermined molecular weight.

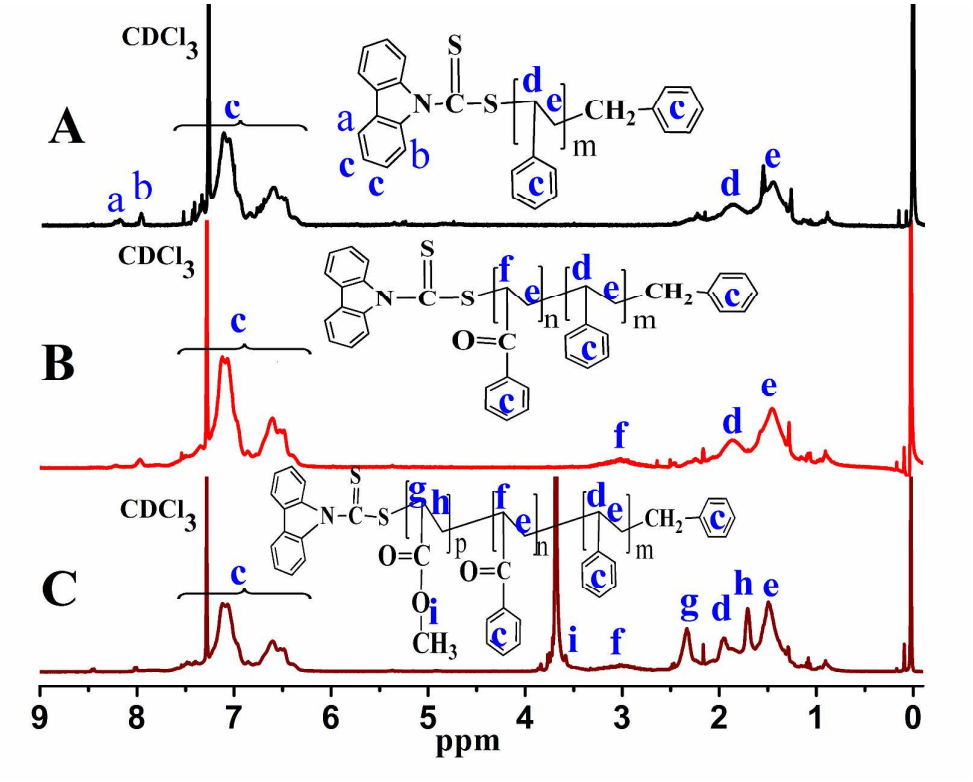

Figure 1. ^{1}HNMR spectra of PSt_{92} (**A**), PSt_{92}-$PPVK_{11}$ (**B**), PSt_{92}-$PPVK_{11}$-PMA_{88} (**C**) in $CDCl_3$

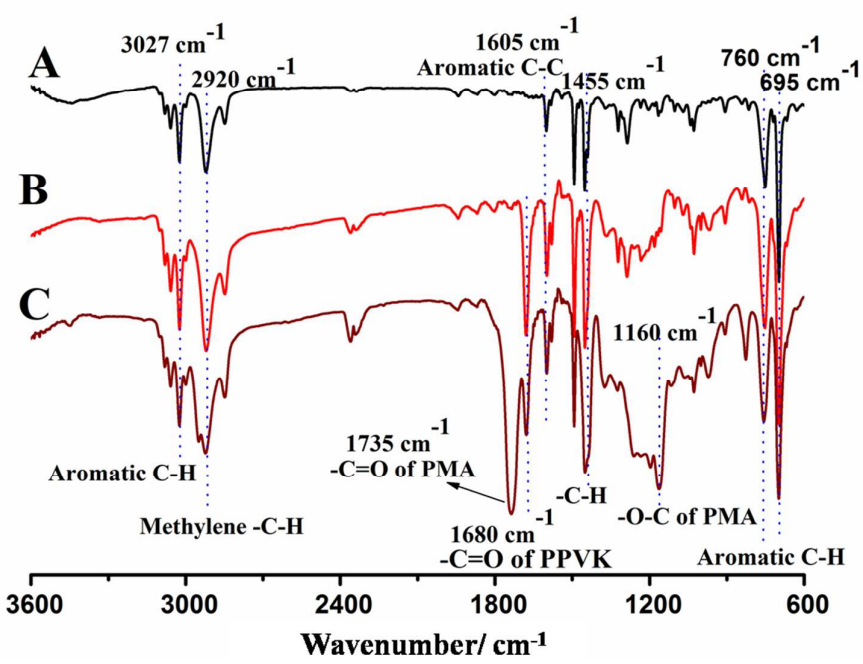

Figure 2. FTIR spectra of PSt_{92} (**A**), PSt_{92}-$PPVK_{11}$ (**B**), PSt_{92}-$PPVK_{11}$-PMA_{88} (**C**)

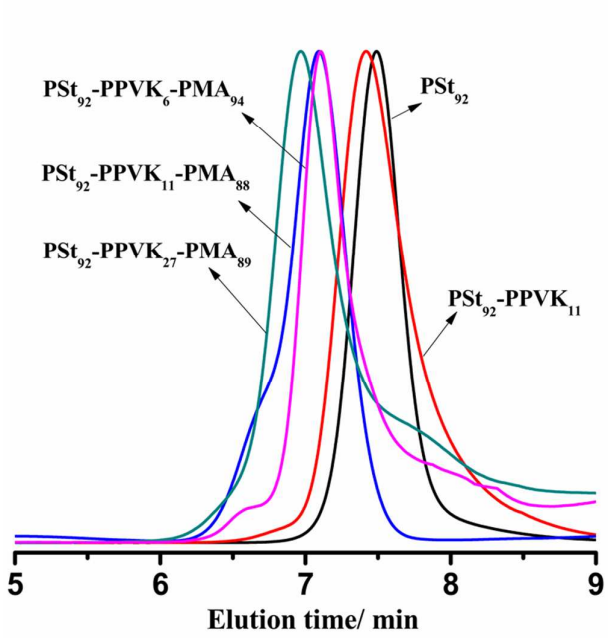

Figure 3. GPC curves of PSt_{92}, PSt_{92}-$PPVK_{11}$, PSt_{92}-$PPVK_6$-PMA_{94}, PSt_{92}-$PPVK_{11}$-PMA_{88} and PSt_{92}-$PPVK_{27}$-PMA_{89}

Table 1. Characteristic data of macro-RAFT agents and triblock copolymers

Sample [a]	M_n [a]	M_n [b]	PDI [b]
PSt_{92}	9901	10150	1.12
PSt_{92}-$PPVK_6$	10693	10940	1.17
PSt_{92}-$PPVK_{11}$	11313	11600	1.18
PSt_{92}-$PPVK_{27}$	13465	13720	1.21
PSt_{92}-$PPVK_6$-PMA_{94}	18777	19050	1.29
PSt_{92}-$PPVK_{11}$-PMA_{88}	18881	18980	1.26
PSt_{92}-$PPVK_{27}$-PMA_{89}	21119	20850	1.28

[a] DP_n was calculated from ^{1}HNMR data; [a] M_n was calculated from ^{1}HNMR data; [b] M_n and PDI were estimated by GPC and calibrated with PSt

Determination of elution order in GPEC

Our previous studies have confirmed that GPEC can be used to separate polymer sample into monomers, additives, oligomers and polymer molecules according to molar mass, chemical composition and functional end group.[35,42] The normal phase GPEC chromatograms recorded by a UV detector at 260 nm of St, PSt_{92}, PMK, PVK,

$PPVK_{48}$, PSt_{92}-$PPVK_{11}$ and PSt_{92}-$PPVK_{11}$-PMA_{88} are shown in **Figure 4**. The UV detector was set at 260 nm corresponding to the UV absorbance of phenyl chromophore (**Figure S6**), allowing the selective detection of St, PMK, PVK, PSt and PPVK block. The GPEC was performed with a combination of a polar silica column and an eluent increasing in polarity using a multistep gradient elution from DCE/ACN = 93/7 (v/v) to DCE/ACN = 30/70 (v/v), which can achieve high resolution. It can be seen from the curves that the PSt, monomer St, PMK and PVK elute at about 2.9 min, 3.3 min, 3.6 min and 3.6 min, respectively. PMK and PVK have very similar retention time under our elution conditions, which may be due to the nearly identical polarity. It was worth pointing out that the molecular weight of PSt has an impact on the retention time of PSt, as the non-interacting PSt chain should elute in the exclusion mode under isocratic conditions.[35-35] Moreover, it can be found from the GPEC chromatograms that the peaks of PPVK, PSt-PPVK and PSt-PPVK-PMA appeared at about 5.4 min, 5.9 min and 9.5 min, respectively. This kind of elution sequence was due to the difference of polarity in PPVK, PSt-PPVK and PSt-PPVK-PMA, which were eluted according to GPEC model based on sorptive interactions between the polymer molecules and the mobile and stationary phases in the column.[36-38] The polarity of PPVK and PMA, especially the PMA segment, is much higher than that of PSt chain, due to the existence of carbonyl and ester groups. As a result, the order of polarity is PSt-PPVK < PPVK <<< PSt-PPVK-PMA. The more polar polymer will interact more strongly with the column stationary phase, and thus its elution will only occur when the polarity of the eluent is sufficiently high. Consequently, PPVK and

PSt-PPVK elute earlier and PSt-PPVK-PMA with highest polarity elutes much later. In sum, the above results indicated that, under the elution conditions used here, sequential elution of different types of polymer chains and monomers was readily achieved, which can be used to study the photocleavage process of PPVK-based triblock copolymers.

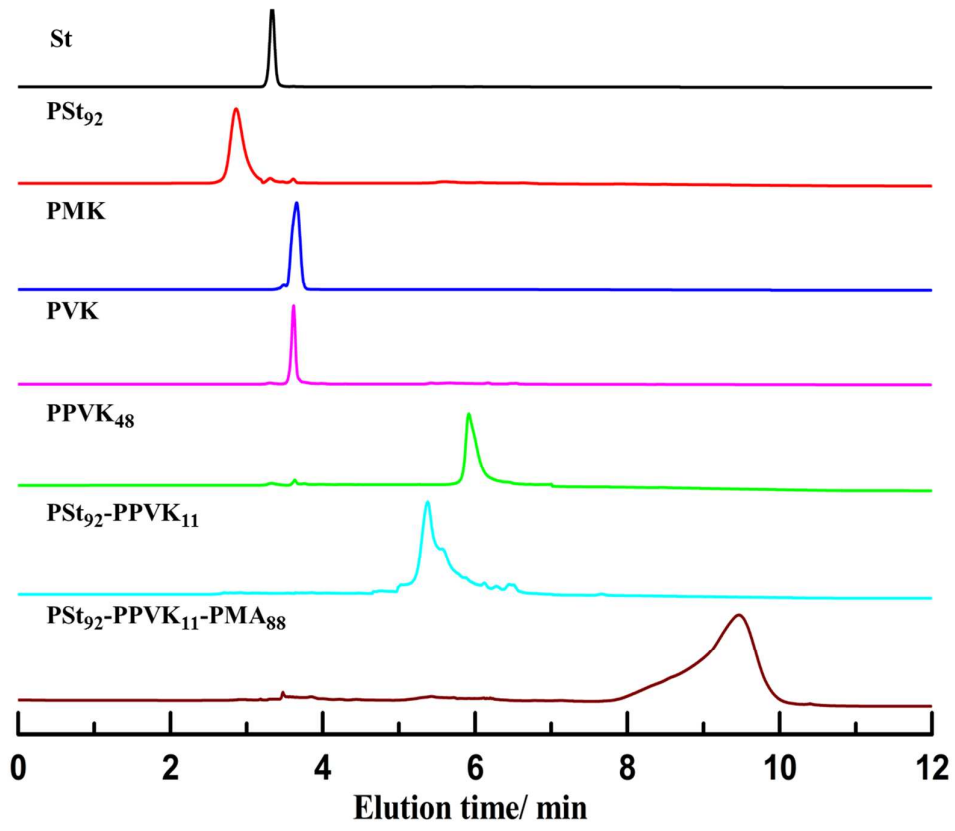

Figure 4. GPEC chromatograms of St, PSt_{92}, PMK, PVK, $PPVK_{48}$, PSt_{92}-$PPVK_{11}$ and PSt_{92}-$PPVK_{11}$-PMA_{88}

Photocleavage process and kinetics of PSt-PPVK-PMA monitored by GPEC

As a type of representative photodegradable polymers, the photodegradation

behaviors and mechanisms of aromatic ketone-based polymers have been studied in detail,[26-30] which revealed that these polymers can undergo a Norrish type II main-chain scission to yield low-molecular weight oligomers, PMK and PVK.[27-29] However, the photodegradation of PPVK-based polymers has never been tracked and quantitatively analyzed. The photocleavage process of PSt-PPVK-PMA was monitored by GPEC and typical chromatograms are shown in **Figure 5**. The identification of the photolysis products of PSt-PPVK-PMA from the GPEC curves of each peak is based on the elution order of the compounds in **Figure 4**. The elution peak of PSt, PMK and PVK, PPVK, PSt-PPVK and PSt-PPVK-PMA can be observed, indicating that the block of PSt-PPVK-PMA can be degraded into smaller molecular segments after exposure to UV light, due to the photo-induced main chain scissions of the middle PPVK block. Some previous studies have proposed that the mechanism of the PPVK photolysis is on the basis of Norrish type photochemical reactions, which can cause a rupture of the C-C backbone, resulting in the formation of PMK and PVK, PPVK and PSt-PPVK.[25-29] Moreover, it should be reasonable to infer that one repeat unit in PPVK block undergoing photolysis reaction will lead to a disconnection of the polymer chain and a decrease in the average molecular weight of the polymer. In addition, upon closer inspection of **Figure 5**, it can be found that the peak of PSt-PPVK-PMA in the GPEC curve after UV exposure 300 s was found to shift from 9.5 min to 10.3 min and meanwhile become much broad. These results indicated most of PSt-PPVK-PMA was completely photodegraded. The peak centered at about 10.3 min can be assigned to PPVK-PMA, indicating the formation of PPVK-PMA, as

PPVK-PMA has longer retention time due to its stronger polarity when compared with PSt-PPVK-PMA. It is worth pointing out that the photolysis products should also include a fraction of PMA, but PMA cannot be observed in the GPEC chromatograms due to PMA without any UV absorbance at 260 nm. Besides, PMA should have the longest retention time because of its strongest polarity. In addition, it can be seen a significant decrease in the relative peak intensities of PSt-PPVK-PMA with the increase of UV exposure time, but a marked increase in the peak intensities of PSt and PMK&PVK. Moreover, compared to the increase in the peak intensities of PMK and PVK, the change of peak intensities of PSt-PPVK and PPVK can be negligible. The results further indicated that the chain scission of PPVK in PSt-PPVK-PMA was the main degradation process, leading to the consumption of PPVK and thus the yield of PMK and PVK. Therefore, these results provide direct evidence for the proposed photocleavage mechanism, as described in Scheme 1 and previously reported by Scaiano et al.[27-28]

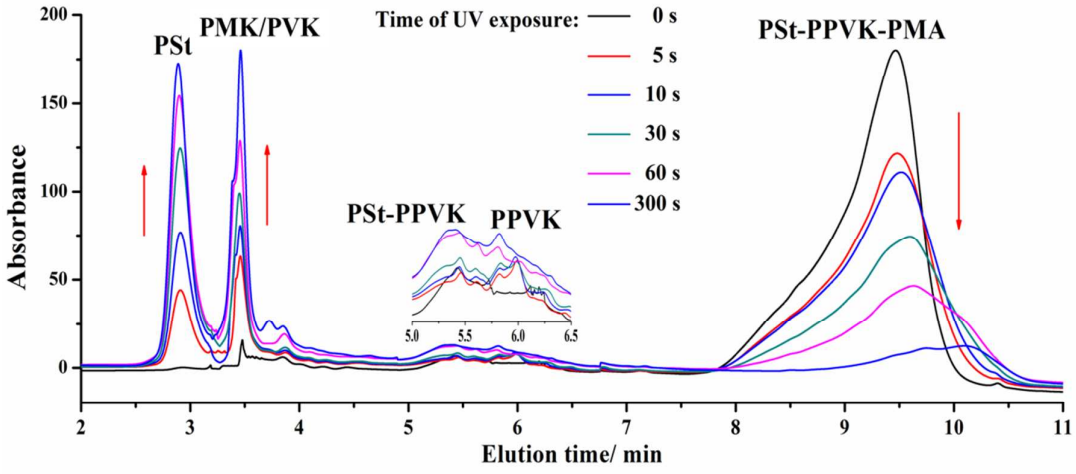

Figure 5. GPEC chromatograms detected at **260** nm of PSt_{92}-$PPVK_{11}$-PMA_{88} after exposure to UV light for different time

The photolysis products of PSt-PPVK-PMA were also determined by GPC, as shown in **Figure 6**. After exposure to UV light, the GPC curves of PSt_{92}-$PPVK_{11}$-PMA_{88} shifted to the lower molecular weight side, suggesting the cleavage of PSt-PPVK-PMA. Moreover, it can be seen that the GPC curve of PSt_{92}-$PPVK_{11}$-PMA_{88} after UV exposure 300 s was close to that of PSt_{92}, indicating a rapid and nearly complete cleavage of PPVK in PSt_{92}-$PPVK_{11}$-PMA_{88}, which was in agreement with the above results of GPEC. In order to study the photolysis kinetics of PPVK in PSt-PPVK-PMA, the residue rate of PSt-PPVK-PMA with different PPVK chain length after UV exposure was evaluated by comparison with the peak areas of PSt-PPVK-PMA before and after UV exposure. The chromatograms were deconvoluted and the residue rate of PSt-PPVK-PMA after UV exposure can be calculated on the basis of Eq. (3).

$$\text{Residue rate} = \frac{A_t}{A_0} \times 100\% \quad (3)$$

where A_0 and A_t is the peak area of PSt-PPVK-PMA before UV exposure and after UV exposure for t s, respectively. The photolysis kinetics was evaluated from plots of the residue rate of PSt-PPVK-PMA after UV exposure versus UV exposure time, and the results were shown in **Figure 7**. The graphs presented in **Figure 7** demonstrated that the chain length of PPVK had a significant impact on the photocleavage of PSt-PPVK-PMA. The increase of the PPVK chain length can speed up the photocleavage of polymers. Moreover, it can be found that the photolysis kinetics, especially for PSt_{92}-$PPVK_{11}$-PMA_{88} and PSt_{92}-$PPVK_{27}$-PMA_{89}, seemed to follow a nearly quasi-parabolic manner. The residue rate firstly decreased sharply with the

increase of UV exposure time and then it was followed by a much slower decrease until that a minimum residue rate was reached after UV exposure 300 s. It is worth pointing out that the residue rate after UV exposure 300 s is relatively high. This is due to the fact that the overlapped peak areas of PSt-PPVK-PMA and PPVK-PMA would cause the measured value larger than true value. These results implied that the photocleavage process of PPVK-based polymers can be controlled by modulating the length of PPVK, which may provide a promising platform to prepare photosensitive functional materials for specific applications.

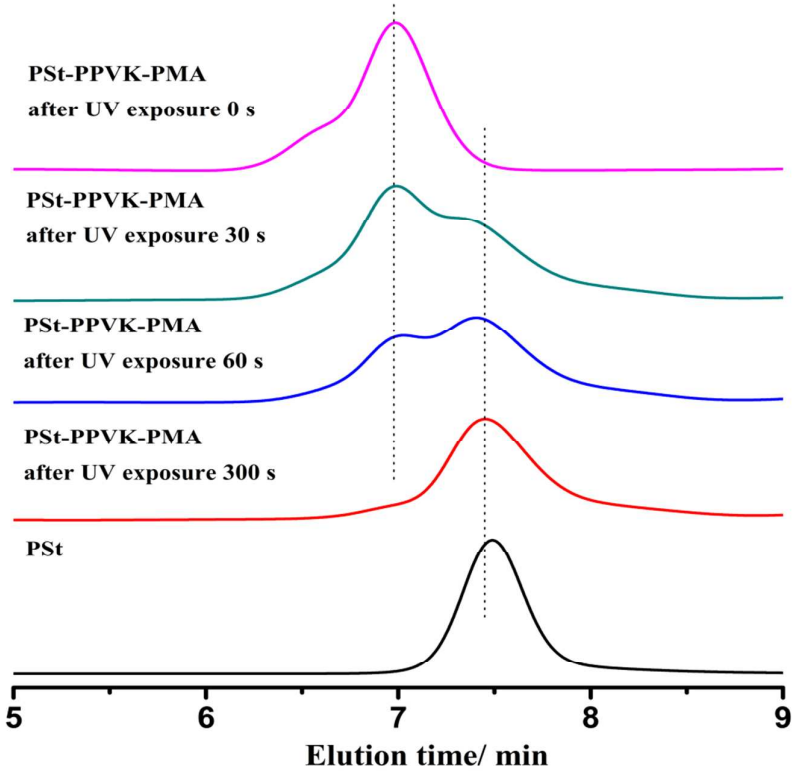

Figure 6. GPC curves of PSt_{92} and PSt_{92}-$PPVK_{11}$-PMA_{88} after exposure to UV light for different time

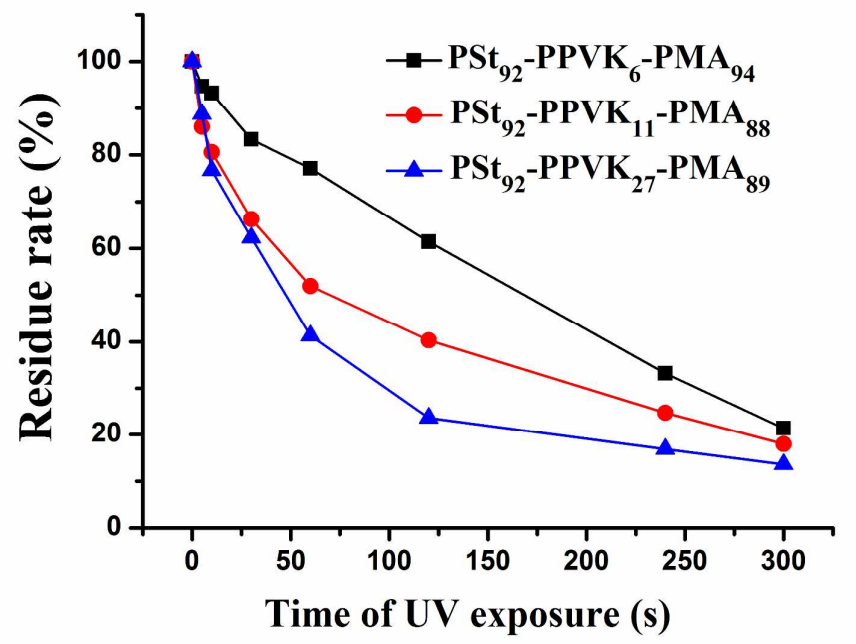

Figure 7. Photolysis kinetics of PSt-PPVK-PMA with different PPVK chain length

Photoresponsive disassembly of PSt-PPVK-PAA micelles

As demonstrated above, the PPVK-based block copolymers with adjustable photocleavable properties can be degraded into smaller molecular fragments under UV exposure, thus leading to significant change in their physicochemical properties and phase behaviors, which have great promise for many applications. In order to demonstrate the photoresponsive properties of PPVK-based polymers, an amphiphilic triblock copolymer PSt-PPVK-PAA and its self-assembled micelles were prepared. The structure and composition of polymers were confirmed by ^{1}HNMR and FTIR (**Figure S2** and **Figure S3**), and the size and morphology of PSt-PPVK-PAA self-assembled micelles in water were characterized by DLS, TEM and AFM. The DLS measurement of PSt-PPVK-PAA micelles was shown in **Figure S7** and the results showed that PSt_{92}-$PPVK_{11}$-PAA_{26} in water could self-assemble into micelles

with an average diameter of about 260 nm. The TEM image in **Figure 8(A)** showed that the PSt-PPVK-PAA micelles were reasonably uniform in size with an average diameter of about 100 nm. The diameter of micelles in a dry state was much smaller than the micelles in water determined by DLS, which should be due to the combined effect of the shrinkage of hydrophilic shells upon drying samples and the highly stretched structure of PAA chains in water because of the mutual repulsion of COO^- groups. TEM observations were also carried out to characterize the morphology change of PSt_{92}-$PPVK_{11}$-PAA_{26} micelles after UV exposure for different time. It can be seen form **Figure 8** that the structures of PSt_{92}-$PPVK_{11}$-PAA_{26} micelles were clearly changed after UV irradiation 2 min. Moreover, no stable polymeric micelles can be observed after UV irradiation 4 min, indicating that PSt-PPVK-PAA micelles underwent relatively rapid disintegration due to the photo-induced cleavage of PPVK in PSt_{92}-$PPVK_{11}$-PAA_{26}. **Figure 9** showed the AFM images obtained from PSt_{92}-$PPVK_{11}$-PAA_{26} micelles solutions before and after UV irradiation 2 min. Before UV irradiation, AFM image showed a high density of spheres. After UV exposure 2 min, the concentration of the spherical micelles markedly decreased, which further confirmed the photo-induced disassembly of micelles. These results conclusively revealed that the amphiphilic PSt_{92}-$PPVK_{11}$-PAA_{26} can self-assemble into well-defined spherical micelles in water, which can be almost entirely disintegrated under UV irradiation due to photocleavage of PPVK in PSt-PPVK-PAA.

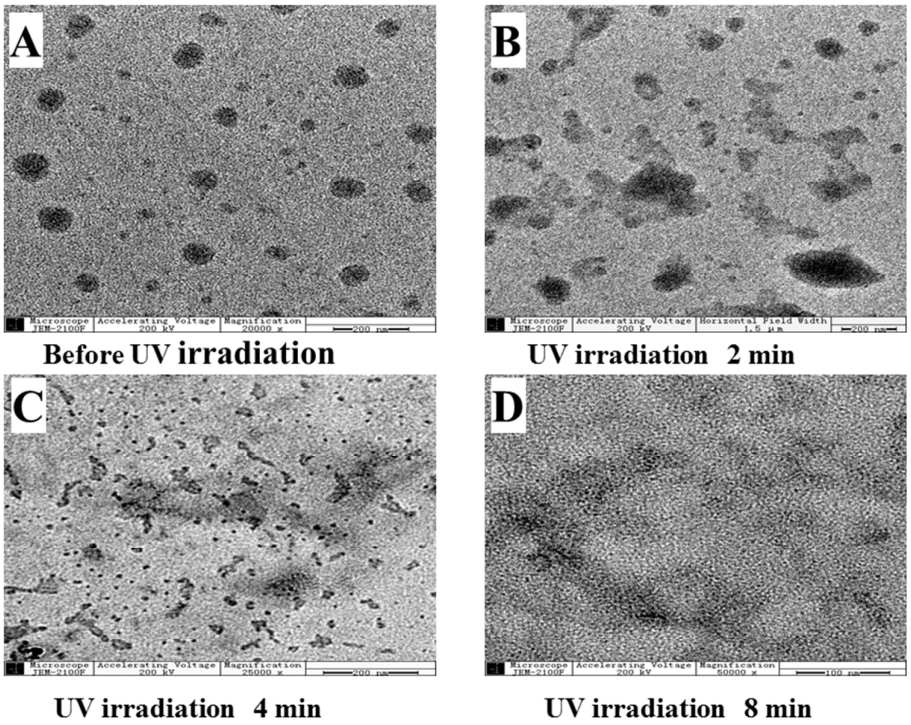

Figure 8. TEM images of PSt_{92}-$PPVK_{11}$-PAA_{26} self-assembled micelles before UV irradiation (**A**) and after UV irradiation 2 min (**B**), 4 min (**C**) and 8 min (**D**)

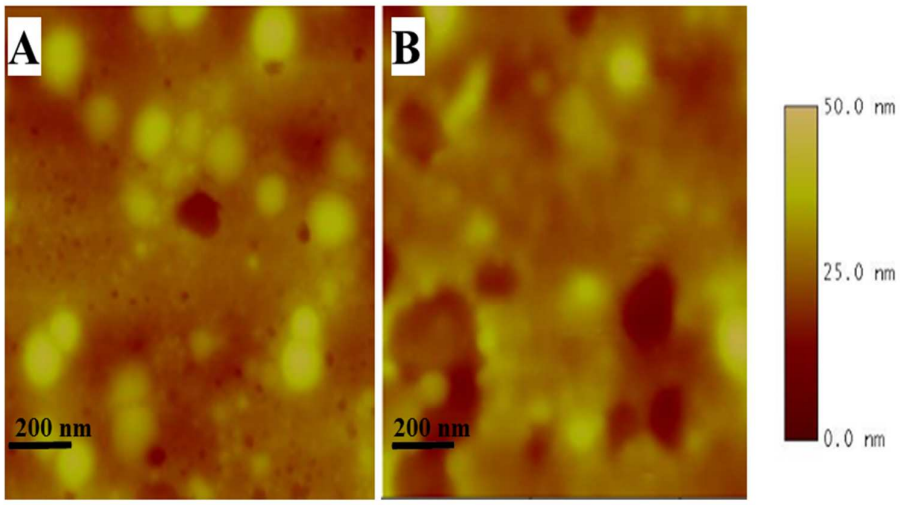

Figure 9. AFM images of PSt_{92}-$PPVK_{11}$-PAA_{26} self-assembled micelles before (**A**) and after UV irradiation 2 min (**B**)

Photo-controllable stabilization of miniemulsions by PSt-PPVK-PAA

One of important applications of amphiphilic block copolymers was used as emulsifiers to stabilize emulsions, due to the excellent tailor-ability of chain structure and thus controllable amphiphilicity.[43-45] The photocleavable PSt-PPVK-PAA was employed as a photoresponsive emulsifier to stabilize water-in-oil miniemulsions. Digital photographs of the miniemulsions stabilized by PSt-PPVK-PAA with and without solar light irradiation were shown in **Figure 10**. Under dark condition, no oil was separated out from the miniemulsions stabilized by PSt-PPVK-PAA, even the miniemulsions were kept for a week. The results indicated that PSt-PPVK-PAA was strongly absorbed at the oil–water interface and showed excellent surface activity. However, as shown in **Figure 10**, under sunlight irradiation, the demulsification occurred and macroscopic phase separation was observed. Moreover, it can be seen that the volume of the oil phase became more transparent and increased with increasing of the time of light exposure. These phenomena indicated that the adsorption of polymeric surfactants at the oil–water interface was expected to be photo-controllable due to the photo-induced cleavage of PSt-PPVK-PAA. It can be believed that this kind of photo-controllable surfactivity and emulsifiability of PPVK-based amphiphilic polymers have a great potential for applications in many fields, such as pharmaceutical formulations.

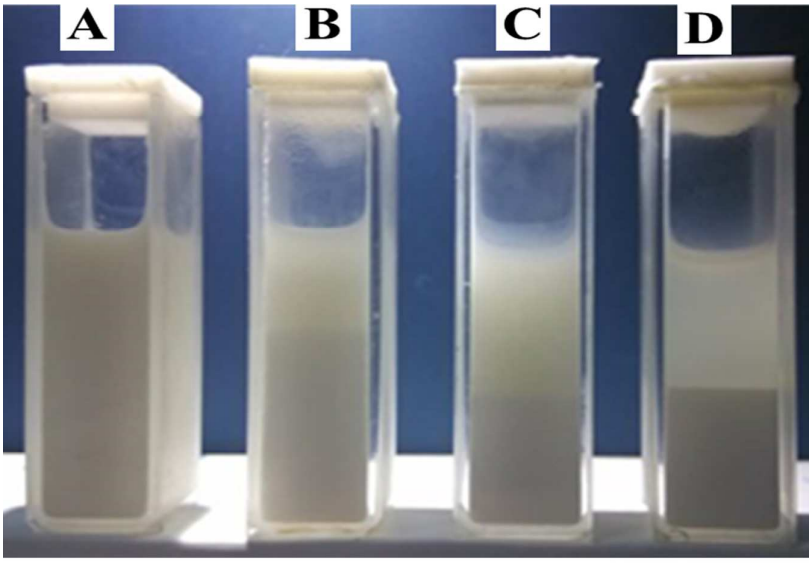

Figure 10. Photographs of W/O miniemulsions stabilized by PSt_{92}-$PPVK_{11}$-PAA_{26} under dark condition for a week (**A**) and under sunlight irradiation for 10 min (**B**), 20 min(**C**) and 40 min (**D**)

Conclusions

In this study, a series of photocleavable well-defined triblock copolymers with the middle block of PPVK, PSt-PPVK-PMA and PSt-PPVK-PAA, were prepared by RAFT polymerization. And then the photocleavage mechanism and kinetics of PSt-PPVK-PMA were systematically investigated by the use of GPEC. The GPEC experiments clearly revealed that the photolysis products of PSt-PPVK-PMA can be successfully fractionated out according to the differences in column interactions. The formation of PMK and PVK in the photolysis products was detected by GPEC, which not only provided the direct evidence for the photocleavage of PPVK, but also confirmed that the Norrish type reaction is mainly responsible for the chain scission of PPVK. In addition, the results about photolysis kinetics clearly demonstrated that the photodegradation rate of PSt-PPVK-PMA can be controlled by adjusting the PPVK chain length in block copolymers. Moreover, due to the photocleavage of PPVK, the PSt-PPVK-PAA self-assembled micelles can undergo photo-triggered rapid disassembly and exhibit photo-controllable surfactivity and emulsifiability. These results suggested that the incorporation of the high photocleavable PPVK into block copolymers by RAFT polymerization provides a promising platform for the construction of complex polymeric architectures with controllable photocleavability, which should be particularly attractive for environmental, biological and medicinal applications.

Acknowledgments

This project was supported by the National Natural Science Foundation of China (Number 31470925)

Reference

1 M. A. C. Stuart, W. T. S. Huck, J. Genzer, M. Muller, C. Ober, M. Stamm, G. B. Sukhorukov, I. Szleifer, V. V. Tsukruk, M. Urban, F. Winnik, S. Zauscher, I. Luzinov and S. Minko, *Nat. Mater.*, 2010, **9**, 101-113.
2 A. Nelson, *Nat. Mater.*, 2008, **7**, 523-525.
3 J. Yin, H. Hu, Y. Wu and S. Liu, *Polym. Chem.,* 2011, **2**, 363-371.
4 F. D. Jochum and P. Theato, *Chem. Soc. Rev.*, 2013, **42**, 7468-7483.
5 F. Ercole, T. P. Davis and R. A. Evans, *Polym. Chem.*, 2010, **1**, 37-54.
6 S. Menon and S. Das, *J. Polym. Sci., Part A: Polym. Chem.*, 2011, **49**, 4448-4457.
7 D. Habault, H. Zhang and Y. Zhao, *Chem. Soc. Rev.*, 2013, **42**, 7244-7256.
8 Y. Zhao, *J. Mater. Chem.*, 2009, **19**, 4887-4895.
9 E. Cabane, V. Malinova, S. Menon, C. G. Palivan and W. Meier, *Soft Matter*, 2011, **7**, 9167-9176.
10 O. Green, N. A. Smith, A. B. Ellis and J. N. Burstyn, *J. Am. Chem. Soc.*, 2004, **126**, 5952-5953.
11 P. Klán, T. Šolomek, C. G. Bochet, A. Blanc, R. Givens, M. Rubina, V. Popik, A. Kostikov and J. Wirz, *Chem. Rev.*, 2013, **113**, 119-191.
12 Y. Zhao, *Macromolecules*, 2012, **45**, 3647-3657.
13 J. Cui, O. Azzaroni and A. del Campo, *Macromol. Rapid Commun.*, 2011, **32**, 1699-1703.
14 H. Zhao, E. S. Sterner, E. B. Coughlin and P. Theato, *Macromolecules*, 2012, **45**, 1723-1736.
15 Q. Yan, D. Han and Y. Zhao, *Polym. Chem.*, 2013, **4**, 5026-5037.
16 H. Zhao, W. Gu, M. Thielke, E. Sterner, T. H. Tsai, T. Russell, E. B. Coughlin and P. Theato, *Macromolecules*, 2013, **46**, 5195-5201.
17 H. Zhao, W. Gu, E. Sterner, T. P. Russell, E. B. Coughlin and P. Theato, *Macromolecules*, 2011, **44**, 6433-6440.
18 M. A. Gauthier, M. I. Gibson and H. A. Klok, *Angew. Chem. Int. Ed.*, 2009, **48**, 48-58.
19 S. Yamago and Y. Nakamura, *Polymer*, 2013, **54**, 981-994.
20 W. A. Brauncker and K. Matyjaszewski, *Prog. Polym. Sci.*, 2007, **32**, 93-146.
21 C. Cheng, G. Sun, E. Khoshdel and K. L. Wooley, *J. Am. Chem. Soc.*, 2007, **129**, 10086-10087.
22 S. Wu, L. Wang and A, Kroeger, Y. Wu, Q. Zhang, C. Bubeck, *Soft Matter*, 2011, **7**, 11535-11545.
23 D. Wang, G. Ye and X. Wang, *Macromol. Rapid Commun.*, 2007, **28**, 2237-2243.
24 M. S. Ho and A. Natansohn, *Macromolecules*, 1995, **28**, 6124-6127.

25 J. E. Guillet and R. W. G. Norrish, *Nature*, 1954, **173**, 625-627.
26 K. Suyama, K. Ito and M. Tsunooka, *J. Polym. Sci., Part A: Polym. Chem.*, 1996, **34**, 2181-2187.
27 J. C. Scaiano and L. C. Stewart, *Polymer*, 1982, **23**, 913-917.
28 R. D. Small, and J. C. Scaiano, *Macromolecules*, 1978, **11**, 840-841.
29 W. J. Leigh, J. C. Scaiano, C. I. Paraskevopoulos, G. M. Charette and S. E. Sugamori, *Macromolecules*, 1985, **18**, 2148-2154.
30 K. Sugita, *Prog. Org. Coat.*, 1997, **31**, 87-95.
31 A. Mittal, S. Sivaram and D. Baskaran, *Macromolecules*, 2006, **39**, 5555-5558.
32 J. A. M. Hepperle, H. Luftmann and A. Studer, *J. Polym. Sci. Part A: Polym. Chem.* 2012, **50**, 2150-2160.
33 A. Gregory and M. H. Stenzel, *Prog. Polym. Sci.*, 2011, **37**, 38-105.
34 G. Moad, M. Chen, M. Hcaussler, A. Postma, E. Rizzardo and S. H. Thang, *Polym. Chem.*, 2011, **2**, 492-519.
35 R. Guo, Z. Shi, X. Wang, A. Dong and J. Zhang, *Polym. Chem.*, 2012, **3**, 1314-1321.
36 X. L. Jiang, P. J. Schoenmakers, J. L. J. van Dongen, X. W. Lou, V. Lima and J. Brokken-Zijp, *Anal. Chem.*, 2003, **75**, 5517-5524.
37 X. L. Jiang, A. Van Der Horst, V. Lima and P. Schoenmakers, *J. Chromatogr., A*, 2005, **1076**, 51-61.
38 H. J. A. Philipsen, *J. Chromatogr., A*, 2004, **1037**, 329-350.
39 P. J. C. H. Cools, F. Maesen, B. Klumperman, A. M. Van Herk and A. L. German, *J. Chromatogr., A*, 1996, **736**, 125-130.
40 A. Bugarin, K. D. Jones and B. T. Connell, *Chem. Commun.*, 2010, **46**, 1715-1717.
41 J. Zhang, A. Dong, T. Cao and R. Guo, *Eur. Polym. J.,* 2008, **44**, 1071-1080.
42 Y. Guo, J. Zhang, P. Xie, X. Gao and Y. Luo, *Polym. Chem.*, 2014, **5**, 3363-3371.
43 S. Fujii, Y. Cai, J. V. M. Weaver and S. P. Armes, *J. Am. Chem. Soc.*, 2005, **127**, 7304-7305.
44 J. Gustafsson, H. Ljusberg-Wahren, M. Almgren and K. Larsson, *Langmuir*, 1997, **13**, 6964-6971.
45 J. Bae, T. P. Russell and R. C. Hayward, *Angew. Chem. Int. Ed.* 2014, **53**, 8240 – 8245.